PRINTED MEMS MEMBRANE ELECTROSTATIC MICROSPEAKERS

Apoorva Murarka, Annie Wang, Joel Jean, Jeffrey H. Lang, and Vladimir Bulovic
Massachusetts Institute of Technology, Cambridge, Massachusetts, USA

ABSTRACT

We report the fabrication and operation of *electrostatic* microspeakers formed by contact-transfer of 125-nm-thick gold membranes over cavities patterned in a micron-thick silicon dioxide (SiO_2) layer on a conducting substrate. Upon electrostatic actuation, the membranes deflect and produce sound. Additionally, membrane deflection upon pneumatic actuation can be used to monitor pressure. Our microspeaker fabrication process enables fabrication of MEMS diaphragms without wet or deep reactive-ion etching, thus obviating the need for etch-stops and wafer-bonding. It enables monolithic fabrication of multiple completely-enclosed drum-like structures with non-perforated membranes to displace air efficiently, in both individual-transducer and phased-array geometries. The microspeaker consumes 262 μW of real electric power under broadband actuation in free field, and outputs 34 dB(SPL/Volt) of acoustic pressure at 10 kHz drive. The microspeaker sound pressure level increases with frequency at 40 dB/decade. The total thickness of the microspeakers is dominated by the silicon wafer substrate (~500 μm thick), with the active device thickness of less than 2 μm. These thin microspeakers have potential applications in hearing aids, headphones, and large-area phased arrays for directional sound sources.

INTRODUCTION

Electrostatically actuated capacitive speakers can have high power efficiency. Electrostatic 30-nm-thick graphene speakers in a single transducer configuration were demonstrated by Zhou *et al*. [1]. There, a single graphene diaphragm was formed on nickel foil using high temperature (1000 °C) chemical vapor deposition, and released from the nickel foil via an iron(III) chloride chemical etch. In contrast, we reported room-temperature, etch-free, contact-transfer printing processes for electrostatically actuated, suspended metal membranes on viscoelastic and flexible substrates [2], and on SiO_2 substrates [3]. However, in these early demonstrations, the acetone-assisted contact-transfer method reported in [3] had low device yield for gold membranes larger than 0.8 mm^2 in area, while the stiction of those membranes to cavity bottoms prevented audible sound production by further decreasing the membrane area available for air displacement. These challenges have been overcome in the present study which reports the modified acetone-assisted contact-transfer method that increases the area of transferred gold membranes to 12.5 mm^2 (covering ~16000 25-μm-diameter cavities), and enables the release of membrane areas stuck to cavity bottoms. This increases the total deflectable area of the membranes, enabling demonstration of audible sound production by *electrostatic actuation*. Alternatively, this microcavity array can be used to sense pressure. We note that the additive fabrication of these contact-transferred membranes removes the need for holes typically found in MEMS diaphragms for etching the underlying sacrificial layer.

DEVICE DESIGN

Our variable-capacitance microspeaker comprises an array of 25-μm-diameter circular cavities in a SiO_2 dielectric layer deposited on a conductive silicon substrate. The cavities are bridged by a 125-nm-thick gold membrane which forms a deflectable top electrode. Deflection of this membrane in response to an applied voltage or an applied pressure can be used to produce sounds or sense pressure. The gold membrane, 12.5 mm^2 in area, covers about 16000 of the 25-μm-diameter circular cavities which are biased simultaneously to respond in parallel, hence enabling the production of a detectable sound pressure level under actuation. The circular cavities are hexagonally-close-packed (as shown in Figure 2) to minimize the non-active capacitance from the underlying SiO_2 supports. The gold electrode is in the shape of a parallelogram (see Figure 2).

FABRICATION

Pick-up Stamp Substrates

The pick-up stamp comprises the cavity-patterned substrate onto which the gold membranes are additively fabricated via lift-off from a transfer pad. A silicon wafer which forms the back electrode of the microspeaker is cleaned in Piranha solution. A 1.1 micron thick SiO_2 layer is deposited on the wafer using plasma-enhanced chemical vapor deposition (PECVD). Hexamethyldi-silazane is then applied to the oxide layer. Photoresist is spun on the oxide layer and pre-baked at 95°C for 30 minutes. The photoresist is then exposed in a mask aligner and exposure unit, using a chrome mask. Following exposure, the photoresist is developed and then baked at 120 °C for 30 minutes. The resulting resist layer has circular patterns, with the underlying SiO_2 exposed; see Figure 1. The exposed SiO_2 is dry etched in tetrafluoromethane/hydrogen (CF_4/H_2) to form ~25-μm-diameter circular cavities. The resist is ashed away in O_2. A thin (60-100 nm thick) insulating layer of SiO_2 is then deposited via PECVD to prevent shorting between the gold membrane and the bottom electrode in case of membrane collapse during electrical actuation. The wafer is diced, cleaned, and exposed to O_2 plasma for 5 minutes. The diced chips are then placed in a 1:5 (by volume) solution of 3-mercaptopropyltrimethoxysilane (Sigma-Aldrich) and 2-Propanol at 80 °C to 100 °C to silanize the SiO_2 surface such that thiol groups stick out of the oxide surface, enhancing the adhesion of gold to the oxide. Upon silanization, these pick-up stamp slides are rinsed with 2-Propanol, and then blown dry using nitrogen, immediately prior to the transfer of the gold membrane.

Transfer Pad with Raised Mesas for Gold Membrane Transfer

The reusable master mold that defines the transfer pad geometry is fabricated using SU-8 photoresist (SU-8 3010 MicroChem) spun onto a silicon wafer and pre-baked at 95 °C for 5 minutes. The wafer is then cooled for 2 minutes before the resist is exposed in a UV exposure unit with a transparency mask. After a post-exposure bake at 95 °C for 2 minutes, the photoresist is developed by immersing and agitating the wafer in propylene glycol monomethyl ether acetate (PGMEA) for 4 minutes. Next, the residual SU-8 and PGMEA are rinsed off by spraying the wafer with PGMEA and 2-Propanol in sequence, for 10 seconds each. The wafer is blown dry with nitrogen and hard-baked for >3 hours at 150-175 °C. Following the hard bake, the master mold is silanized with trichloro(1H,1H,2H,2H-perfluorooctyl)silane (Sigma-Aldrich) to ensure easy removal of PDMS that is next cured on top of it [6].

The PDMS transfer pad is molded by pouring a degassed mixture of PDMS (Sylgard 184, Dow Corning Co., 10:1 base-to-

9781940470016/HH2014/$25©2014TRF

Solid-State Sensors, Actuators and Microsystems Workshop
Hilton Head Island, South Carolina, June 8-12, 2014

curing-agent ratio by weight) onto the silanized SU-8 master mold, and curing it in an oven at 60-105 °C for ~37 hours. The cured PDMS pad is peeled from the SU-8 master. This pad has parallelogram-shaped mesa structures that rise above the plane of the PDMS substrate and aid the patterning and transfer of the metal electrodes since thermal evaporation is a line-of-sight process [6]; see Figure 1. After curing, a ~20 nm thick layer of aluminum is thermally evaporated on the PDMS transfer pad to prevent any cracks in the underlying PDMS substrate from adversely affecting the topography of the gold films to be deposited, and to slow down the diffusion of TPD into the PDMS substrate. The transfer pad is then exposed to O_2 plasma for 7 seconds, after which a 90 nm thick organic release layer of *N*,*N*'-diphenyl-*N*,*N*'-bis(3-methylphenyl)-(1,1'-biphenyl)-4,4'-diamine (TPD, Luminescence Technology Co.), and a 125 nm thick layer of gold are deposited in sequence via thermal evaporation onto the transfer pad [2]. The vacuum-evaporated gold film above the mesas is much thinner than the height of the mesas. Thus, the gold film breaks along the edges of the mesas and defines a film in the shape of the mesa plateaus with sub-micron edge roughness.

Contact Lift-Off Transfer

Following thermal evaporation, the TPD layer underneath the parallelogram-shaped gold membranes is dissolved by applying 60-100 µL of acetone to a ~1 cm^2 area on the transfer pad. Gold membrane transfer is then initiated by placing the pick-up stamp in contact with the gold membranes, which are still resting on the mesas of the transfer pad. The gold membranes adhere to the MPTMS-treated pick-up stamp upon conformal contact, and are lifted-off. The transferred gold membranes cover the circular air-cavities in the stamp, forming the top electrode of the microspeaker, as shown in Figure 2. The device can then be heated on a hot plate from 100 °C to 260 °C over 30 minutes to release the areas of the transferred gold membrane that have sunk into the underlying cavities.

TEST RESULTS

The yield of the aforementioned MEMS fabrication process can be quantified by the fraction of the area of the transferred gold membrane (of a device) that has not sunk into the cavities in the underlying substrate since that is the active area of the membrane responsible for displacing air during the electrostatically-actuated production of sound. Excessive pressure applied during the contact-lift-off transfer process likely results in the gold membrane coming into contact with the bottom of some cavities. Possible reasons for the membrane then sticking to the bottom are the presence of MPTMS in the cavity wells or acetone-enabled stiction [3]. Increasing the thickness of the silicon dioxide spacer layer decreases the sunk-in area of the transferred membranes, but increases the voltage required to achieve sufficient sound production. Heating the device after membrane transfer, as described above, releases a significant fraction of the sunk-in membrane areas. However, some areas of the transferred membrane remain sunk-in even after the heat treatment, and do not contribute to the production of sound.

The mechanical deflection of the gold membrane is first characterized using optical interferometry. Electrical contact to the gold membrane is made using gold-wire probe tips. A 1 kHz sinusoidally-varying voltage with a 60 V peak-to-peak amplitude and a 30 V DC bias is applied between the gold membrane and the silicon substrate. The resulting deflection of the membrane over the underlying cavities is measured at different phases of the applied signal using an optical interferometer (Wyko NT9100, Bruker Nano Inc.). As the phase of the applied signal increases

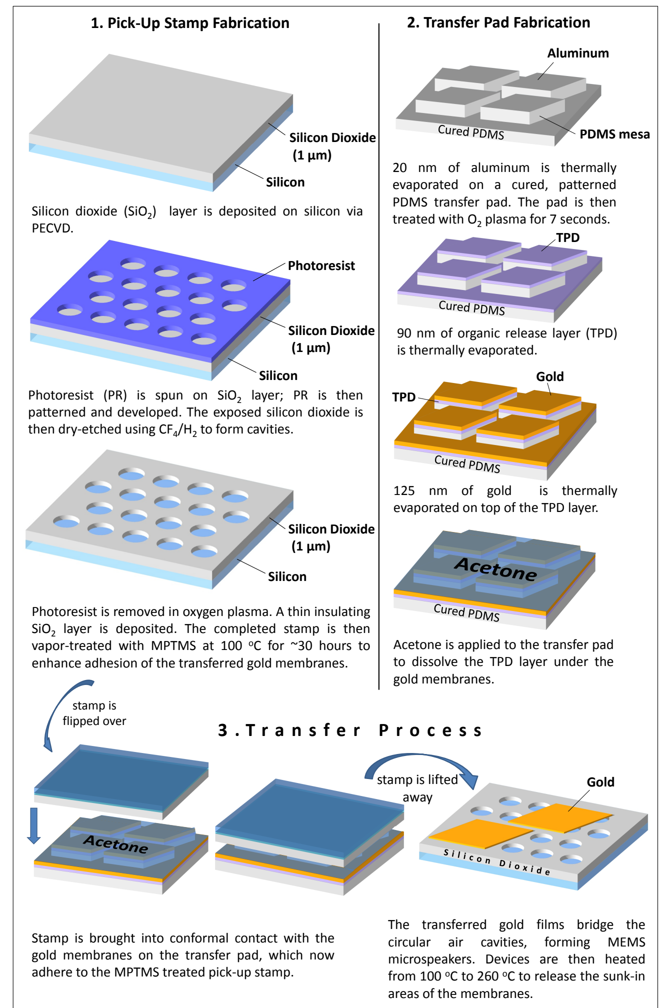

Figure 1: The process flow for the acetone-assisted, contact-transfer MEMS printing process on silicon-based substrates. The drawings above are not to scale.

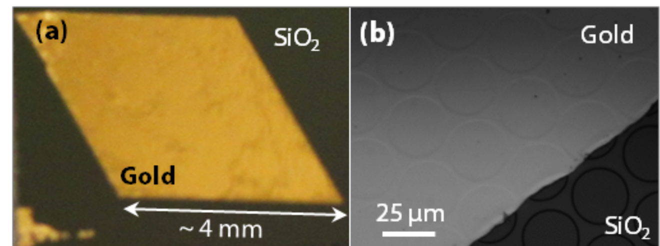

Figure 2: Photographs of large area gold membranes contact-transfer printed on SiO_2 dielectric layers patterned with ~25-µm-diameter cavities to form MEMS microspeakers. (a) A single 12.5-mm^2-area gold membrane covering ~16000 circular cavities, in an individual-transducer configuration. (b) An optical microscopy image of a similar MEMS device, showing a gold membrane bridging several 25-µm-diameter cavities in SiO_2.

from 270° to 90° (450° mod 360°), the voltage between the gold membrane and the underlying substrate increases. As a result, the electrostatic force of attraction between the membrane and the underlying electrode increases, resulting in an increasing downward deflection at the center of the suspended membrane, as shown in Figure 3a (blue triangles); both the applied voltage and deflection are shown. Analysis of the deflection of a gold

membrane over 83 different cavities reveals a repeatable maximum deflection of 121±13 nm across gaps of ~25 microns at 60 V. Figure 3b shows the same data with time as a parameter. However, squared voltage (which is proportional to force) is displayed instead of voltage. Since the membrane deflections are believed to be elastic and recoverable, a linear relation between the applied electrostatic force and the maximum membrane deflection should be observed. The electrostatic force scales with the square of the applied voltage assuming that maximum membrane deflection is small compared to the initial distance between the membrane and the underlying silicon electrode. As a result, one can expect the maximum membrane deflection to scale approximately with the square of the applied voltage, and this is observed in the linear relationship in Figure 3b. However, that graph also shows that the energy conversion cycle encloses net area, which indicates that net electrical energy is converted to mechanical energy. This may result from radiated sound or irrecoverable deformations in the membrane.

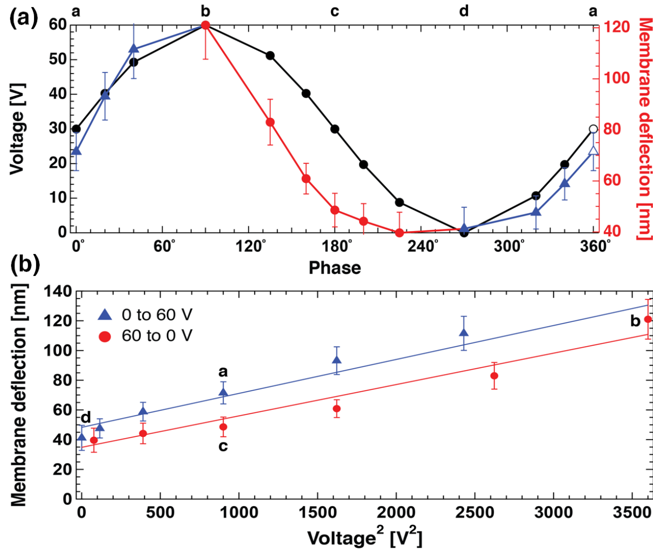

Figure 3: Deflection profiles of a gold membrane suspended over cavities, obtained via optical interferometry during 1 kHz AC actuation. The peak (center) deflections of this membrane over 83 cavities as functions of time were extracted from the profiles and then averaged to yield a single deflection time function. That time function and the corresponding applied voltage are shown here. (a) The applied voltage (black) and the averaged peak membrane deflection (red and blue) are shown as functions of time. (b) The membrane deflections are plotted against the square of the applied voltage with time as a parameter. The points labeled a-b-c-d-a in (b) indicate the position of corresponding points on the periodic deflection and voltage waveforms in (a).

The acoustic performance of the microspeakers is characterized in the free-field using different types of actuation signals such as normally distributed pseudorandom noise signals and chirp signals in the human auditory range. The setup for these tests is shown in Figure 4.

Bandlimited and broadband noise signals are applied as voltages to the microspeaker, at Bose Corporation, under computer control via an audio interface (RME Fireface 800) and a high voltage amplifier. The sound produced in the free field is measured and recorded using a Brüel & Kjær (B&K) 4135 microphone at an on-axis distance of ~4 mm from the devices. The B&K 4135 is a reference microphone with a flat frequency response from 10 Hz to

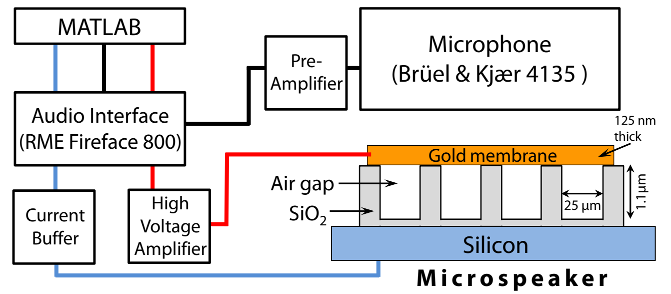

Figure 4: Schematic of the setup used for acoustic characterization of the microspeaker. Signals generated by MATLAB are amplified and applied to the microspeaker to actuate it electrostatically. The resulting generated pressure is sensed using the microphone, and fed back to MATLAB for subsequent processing and analysis.

20 kHz. The current through the microspeaker is simultaneously measured via a current buffer.

Two types of normally distributed pseudorandom noise signals are applied to a device with 12.5-mm^2-area gold membrane. The first input signal is broadband noise from 100 Hz to 22 kHz, biased at 35V, with a standard deviation of ~8 V and a peak deviation of ~35 V (as shown in Figure 5 inset). The second input signal is bandlimited using a third-order Butterworth bandpass filter between 2 kHz and 7 kHz, with a roll-off to ~22 kHz, biased at 35 V. The transfer function, T_{pv}, from the driving voltage, v, to the sound output, p, measured by the microphone is computed as the ratio S_{pv}/S_{vv}, where S_{pv} is the cross-spectral density between p and v, and S_{vv} is the autospectral density of v. The transfer function magnitudes obtained from these measurements

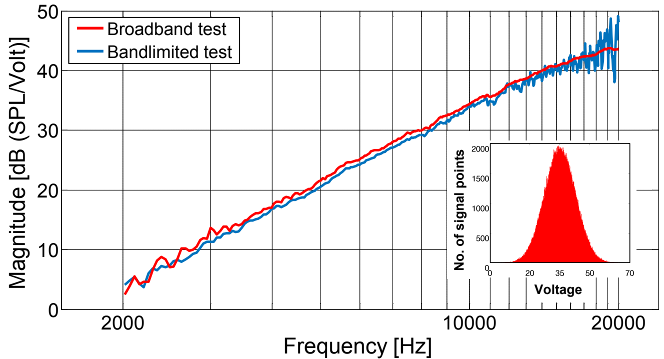

Figure 5: Acoustic frequency response, from 2 kHz to 20 kHz, of a gold membrane microspeaker, 12.5 mm^2 in area. The magnitude of the transfer function, $|T_{pv}|$, from the driving voltage amplitude to the sound output measured by the microphone is converted to decibels using 20 μPa as the reference pressure, i.e., the magnitude plotted is $20log_{10}(|T_{pv}|/20\mu Pa)$. *Inset: Histogram of the normally distributed broadband driving signal amplitudes.*

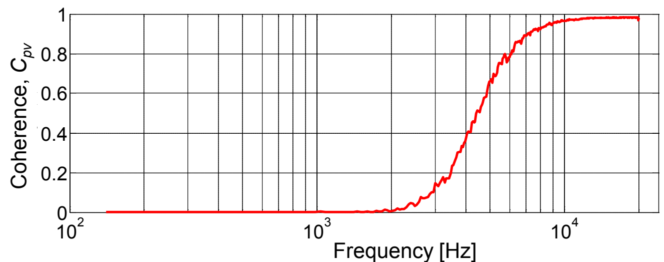

Figure 6: Spectral coherence, C_{pv}, between the sound output measured by the microphone and the driving voltage, for the broadband driving signal.

are shown in Figure 5 for frequencies from 2 kHz to 20 kHz because the microphone output is dominated by incoherent noise below 2 kHz for both measurements. The ~40 dB/decade rise of the frequency response in the range shown in Figure 5 indicates that the sound pressure output of the microspeaker is proportional to the acceleration of the microspeaker diaphragm, as expected in the spring-controlled regime for free field radiation. The frequency response to the bandlimited driving signal is noisier near 20 kHz because the energy in the bandlimited signal is much lower near 20 kHz as compared to that in the broadband driving signal. A reference pressure of 20 µPa is used to calculate the sound pressure level (SPL) per Volt in decibels.

The spectral coherence, C_{pv}, between the sound output and the broadband driving voltage signal is shown in Figure 6, from 100 Hz to 20 kHz. C_{pv} is nearly zero for frequencies less than 2 kHz. Over this range, the recorded sound signal is likely dominated by background noise because the microspeaker signal is weak at low frequencies. Note that the microspeaker pressure output in the free field is proportional to the diaphragm acceleration which is lower at lower frequencies in the spring-controlled regime in which the microspeaker is actuated. The microspeaker response is linear above 10 kHz (C_{pv} > 0.97) for the normally distributed broadband driving signal.

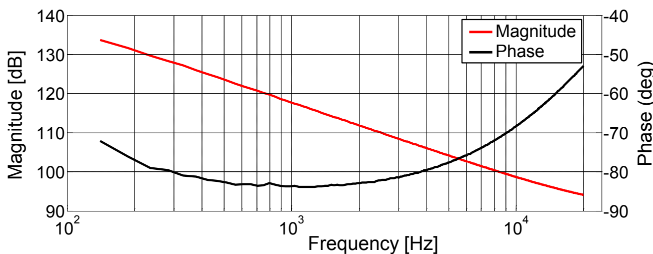

Figure 7: Magnitude and phase of the microspeaker electrical impedance obtained from the broadband test. The ~18 dB/decade decrease in magnitude indicates the primarily capacitive nature of the microspeaker (~200 pF). The reference impedance is 1 Ohm.

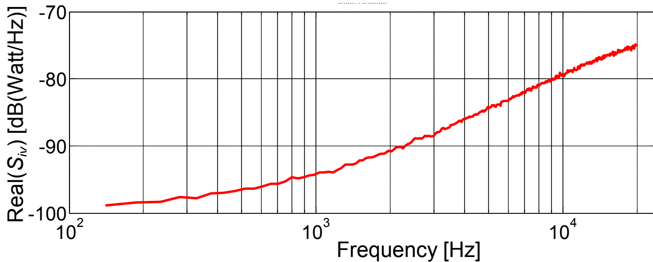

Figure 8: Real part of the cross spectral density, S_{iv}, between the microspeaker current and the driving voltage, for the broadband driving signal. The magnitude plotted is $10log_{10}$(Real(S_{iv})). The reference power spectral density is 1 Watt/Hz.

The electrical impedance of the microspeaker is shown for the broadband measurement in Figure 7. The ~18 dB/decade decrease of the impedance magnitude indicates that the microspeaker device is primarily capacitive near 200 pF during the broadband operation. Additionally, the impedance phase increase from -84 degrees at 1 kHz to -53 degrees at 20 kHz indicates the presence of a 30 kΩ series resistance. This resistance is too high to be explained by the resistivity of the membrane and the substrate.

The magnitude of the real part of the cross-spectral density, S_{iv}, between the driving voltage, v, and the current, i, through the microspeaker for the broadband driving signal is shown from 100 Hz to 20 kHz in Figure 8. Integrating this curve from 100 Hz to 20 kHz yields 262 µW as the real electric power input to the microspeaker during broadband excitation.

The frequency response of the microspeakers can potentially be improved, especially at the lower frequencies, by combining cavities of larger diameters in parallel, under a single gold diaphragm. The SPL output of the microspeakers can also be increased by using membranes of larger area that displace a larger volume of air, or by actuating multiple smaller membranes simultaneously on the same die. The actuation voltage can be reduced by using a thinner dielectric spacer layer between the gold membrane and the bottom electrode, but this could adversely affect the yield. Additionally, the efficacy of these devices in portable audio applications such as hearing aids and earphones can be better gauged by measuring the acoustic characteristics in a pressure field using a coupling cavity (of 2 cm^3 volume) between the microspeaker and the microphone.

CONCLUSION

A contact-printed electrostatic MEMS microspeaker is demonstrated. It comprises a 125-nm-thick deflectable gold membrane suspended over an array of ~16000 circular cavities patterned in a 1.1-micron-thick dielectric layer. Each cavity is 25 µm in diameter. Its electromechanical performance under AC actuation is characterized via optical interferometry to show a repeatable maximum deflection of 121±13 nm. The microspeaker acoustic response in free field is characterized using normally distributed pseudorandom broadband and bandlimited signals, suggesting potential applications of these microspeakers in hearing aids, earphones, and large-area phased arrays for directional sound sources.

ACKNOWLEDGEMENTS

The authors gratefully acknowledge and thank Ole Nielsen of Bose Corporation for his assistance with the acoustic characterization tests and for the invaluable discussions. This work is supported by the National Science Foundation (NSF) Center for Energy Efficient Electronics Science (E3S) Award ECCS-0939514. The authors also thank Patrick Brown and Andrea Maurano for assistance rendered. The devices described here were fabricated in the MIT Microsystems Technology Laboratories and the MIT Organic and Nanostructured Electronics Laboratory.

REFERENCES

[1] Q. Zhou and A. Zettl, “Electrostatic graphene loudspeaker,” Applied Physics Letters, 102 (2013).

[2] A. Murarka, C. Packard, F. Yaul, J. Lang, V. Bulovic, “Micro-contact printed MEMS,” Technical Digest of the IEEE MEMS 2011 Conference, Cancun, January 23-27, 2011, pp. 292-295.

[3] A. Murarka, S. Paydavosi, T. Andrew, A. Wang, J. Lang, V. Bulovic, “Printed MEMS membranes on silicon,” Technical Digest of the IEEE MEMS 2012 Conference, Paris, January 29-February 2, pp. 309-312.

CONTACT

*A. Murarka, tel: +1-617-4525403; apoorva@mit.edu